SIMULATING THREE DIMENSIONAL SELF-ASSEMBLY OF SHAPE MODIFIED PARTICLES USING MAGNETIC DIPOLAR FORCES

Laurens Alink [1], G.H. (Mathijs) Marsman [1], Léon A. Woldering [1] and Leon Abelmann [1]

[1] *Mesa+ Institute for Nanotechnology, University of Twente, The Netherlands*

***Abstract* — The feasibility of 3D self-assembly of milli-magnetic particles that interact via magnetic dipolar forces is investigated. Typically magnetic particles, such as isotropic spheres, self-organize in stable 2D configurations. By modifying the shape of the particles, 3D self-assembly may be enabled. The design of the particles and the experimental setup are presented. The magnetic configurations of simple particle arrangements are obtained via energy minimization in simulations. The simulations show that a 3D configuration can become energetically favourable over 2D configurations, if the shape of the particle is modified.**

***Keywords:* 3D self-assembly, magnetism, dipolar forces, anisotropic particles, energy minimization**

I – Introduction

Microfabrication techniques are currently based on top-down lithography and therefore inherently two dimensional (2D), or at best very restricted in the third dimension. Fabrication by means of three dimensional (3D) self-assembly will open up a wide range of new applications, such as new types of (smart) supermaterials with interesting optical, mechanical, electrical and magnetic properties [1]. On the long term, we envision 3D electronics as an answer to atomic limits emerging at the end of Moore's law progress [2].

In this paper, we focus on 3D self-assembly driven by dipolar magnetic forces. Particles that interact by dipolar forces only, typically assemble in 2D configurations preferably [3]. Our approach to overcome this limitation is to enable 3D magnetic self-assemblies by clever design of the shape of the particles. In order to have accurate control over the shape, this approach is investigated using millimeter sized particles. Some simple configurations of milli-magnetic particles are shown in figure 1. We investigate the stability of such simple configurations by means of simulations and extend into non-spherically shaped particles.

Figure 1: *Photographs of simple configurations of toy magnets ('neocubes') with a diameter of 4 mm. All the configurations are stable, except for the two rightmost configurations; when the magnets are forced in one of these meta-stable configurations, they readily rearrange when touched.*

II – Setup and particle design

There are four distinct elements that play a role in all self-assembly systems: (I) the particles, (II) binding forces, (III) driving forces and (IV) the environment. In our case these elements are the following: The particles are millimeter sized plastic shells, which are fabricated by 3D-printing. This fabrication technique allows the shape to be to be controlled in an arbitrary fashion. The particles contain an embedded hard magnet. Consequently, magnetostatic forces are the main binding force. In this case, magnetostatic forces are also driving the self-assembly. To enhance the (random) motion of the particles, a turbulent flow will be induced in the liquid by means of agitation. All experiments will be carried out in an aqueous environment. We intend to have the particles hover, *i.e.*, neither sink nor float in the liquid, thus enabling self-assembly without constraints by the bottom or side walls of the beaker. Therefore, for neutral buoyancy, the density of the liquid will be matched with the density of the particles by dissolving NaCl in the water. The designated experimental setup is schematically depicted in figure 2a.

The milli-magnetic particles are neodymium magnets enclosed in a 3D-printed shape, see figure 2b. The used magnets are off-the-shelf neodymium disc magnets. These magnets have their magnetization oriented along their axis. The design specifications the particles are listed in table 1. The particles are designed such that the maximum magnetic force between two particles is slightly larger than the net downward force in water. In this way, the particles can bond magnetically, but weak bonds can still be broken by supplying energy via the turbulently flowing water. Furthermore, we closely match the density of the particles (1.3 kg/L) and the liquid (1.2 kg/L). Therefore, the downward force will be tuned to a small value. For the first test experiments, the particles have a spherical shape.

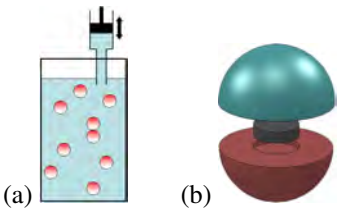

Figure 2: *(a) Schematic drawing of the experimental setup. Shown are the beaker, which contains the liquid with the milli-magnetic particles, and the inlet to which an agitation pump can be connected. (b) Exploded view of a milli-magnetic particle. Shown are the neodymium magnet and the 3D-printed plastic encapsulation, which consist of two half-spheres; their difference in color allows to identify the 'North' and 'South' pole of the particle.*

Table 1: *Design specifications of the particle. In the effective density of the particle, the density and volume of the neodymium magnet and plastic shell are taken into account. The magnetostatic force that is listed here, is the maximum magnetostatic force that two particles can exert on each other [4].*

property	dimension
particle radius, r	5 mm
magnet radius	2 mm
magnet height	1 mm
effective density particle	1.3 kg/L
saturation magnetization, M_s	1.2 T/μ_0
magnetostatic force, F_m	8.3 mN
gravitational force	6.8 mN
net downward force in water	1.7 mN

III – Simulation procedure

The preferred magnetic configuration (that is, the orientations of the magnetic moment of the particles) is found by minimizing the magnetostatic energy of the configuration dynamically. For simplicity, the particles are treated as dipoles. Only the torques on the dipoles are considered and not the forces. In other words, the positions of the particles are fixed in the simulations and the particles can only lower their energy via rotation. We determined stable positions of the particles by using the observed configurations of the neocubes in figure 1 as a guide.

The magnetostatic energy of a single dipole in a magnetic field is given by

$$U = -M\mathbf{m}\cdot\mathbf{B}, \tag{1}$$

where $M = M_s V_m$ is the magnitude of the dipole moment, with V_m the volume of the particle's magnet; $\mathbf{m}$ is the unit vector in the direction of the dipole moment and $\mathbf{B}$ is the magnetic field at the position of the dipole.

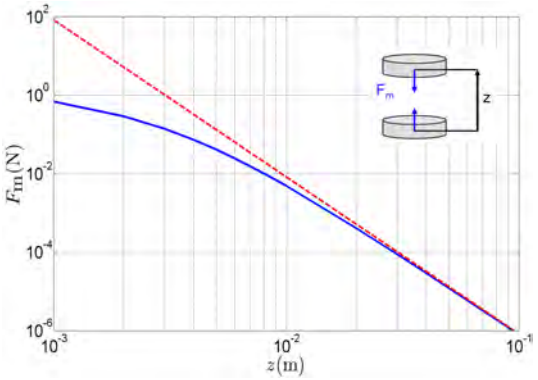

Figure 3: *Force between two cylindrical magnets with a common axis, as a function of center to center separation. The cylinders have an axial magnetization and dimensions as listed in table 1. The exact solution [4] (solid line) and dipole approximation (dashed line) are shown.*

This magnetic field is caused by the other dipoles in the system. The field of a single dipole is given by

$$\mathbf{B} = \frac{\mu_0}{4\pi}\frac{1}{|\mathbf{r}|^3}\left(3\hat{\mathbf{r}}(\mathbf{m}\cdot\hat{\mathbf{r}}) - \mathbf{m}\right), \tag{2}$$

where $\mathbf{r}$ is the distance between the dipole and the point where the field is evaluated and $\hat{\mathbf{r}}$ is the unit vector from the dipole to this point. The magnetostatic force acting on a dipole can be obtained by

$$\mathbf{F} = -\nabla U. \tag{3}$$

In figure 3, the forces between two dipoles are compared with the forces between cylindrical shaped magnets. At large distances, the dipole approximation is accurate. However, the approximation is less accurate at distances that are comparable to the size of the cylindrical shaped magnets. Therefore, the accuracy of the simulations can be improved by taking the exact fields into account for nearest neighbour particles.

The total magnetostatic energy of a configuration of particles can be obtained by summing the energies of all the dipoles in the system.

The magnetostatic energy is minimized by allowing the dipole moments to rotate in the direction of the net field via

$$\frac{\Delta\mathbf{m}}{\Delta t} = -\alpha\,\mathbf{m}\times(\mathbf{m}\times\mathbf{H}), \tag{4}$$

with $\mathbf{H} = \mathbf{B}/\mu_0$. After each iteration step Δt, a new configuration of the dipole moments is calculated with its resulting field. The damping factor α is manually adjusted to optimize simulations speed while maintaining convergence. The simulation is stopped after 10000 steps, or when the change in the total magnetization is below a certain tolerance:

$$\sum_{n=1}^{N} |\Delta\phi_n| + |\Delta\theta_n| < 10^{-5}\ \text{rad}, \tag{5}$$

where N is the number of dipoles in the configuration and ϕ and θ are the angles defining the direction of dipole moment; $\Delta\phi$ and $\Delta\theta$ are the changes of these angles in a single time step.

The energy does not necessarily converge to a global minimum. Therefore, the simulations are repeated several times, with random initial dipole moments, to find the magnetic configuration with the lowest energy.

IV – Results and discussion

The energies corresponding to the simple configurations in figure 1 have been simulated first. The distance between two neighbouring particles in these configurations is $2r$. Table 2 shows the final magnetization state of the simple configurations and the corresponding energies. The energies scale with M^2. The configuration with the lowest energy for $N = 3$ is the 'line' configuration in 3.a. For $N = 4$ the 'ring' configuration in 4.b has the lowest energy.

Table 2: *Magnetic configurations and normalized magnetostatic energies after energy relaxation; in all configurations the dipoles are positioned in plane, except for the 3D configuration 4.d*

configuration		magnetostatic energy U/M^2 J$(Am^2)^{-2}$
3.a		−0.85
3.b		−0.75
4.a		−1.31
4.b		−1.34
4.c		−1.28
4.d		−1.00

Configuration 4.c and the 3D configuration 4.d, have higher energy, as was expected from our experience with the neocubes.

A. energy barriers

The energy barrier between configuration 3.a and 3.b has been investigated, see figure 4. The trajectory is parametrized by angle θ, which is defined in the figure. For each θ, the lowest energy state is found via the simulations. Both the 3.a and 3.b configurations correspond to a minimum in the energy landscape. This means that these configurations are stable. The maximum energy is attained for $\theta = 105°$. For the 4-dipole system, two trajectories are considered. In the first trajectory, an in-plane path from configuration 4.b to 4.c is parametrized. The energy corresponding to this trajectory is given in figure 5. At $\theta = 120°$, $U(\theta)$ has a local maximum. Therefore, the configuration of 4.c is not stable. This is in correspondence with the observed meta-stable behaviour of the neocubes in this configuration.

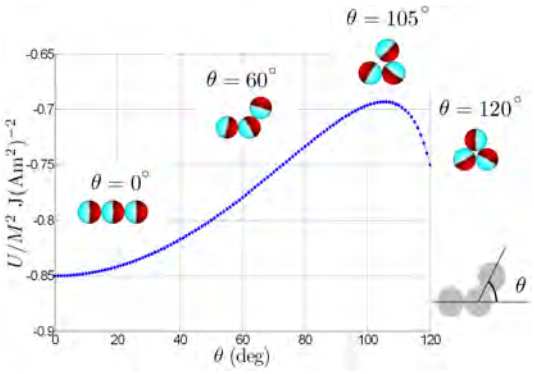

Figure 4: *Trajectory in the energy landscape of a 3-dipole system; the energy is plotted against θ, which is defined in the lower right. The insets show the configuration of the particles for various θ, after minimization of the energy.*

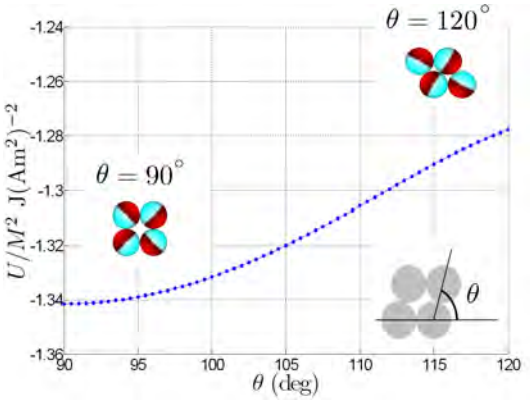

Figure 5: *The in-plane trajectory in the energy landscape of a 4-dipole system. The energy is plotted against θ, which is defined in the lower right inset. The magnetic configurations after energy minimization for $\theta = 90°$ and $\theta = 120°$ are also shown.*

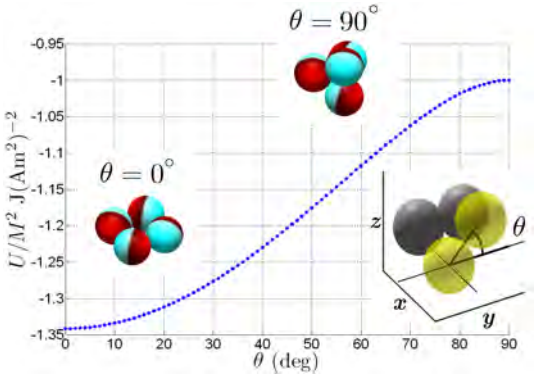

Figure 6: *The out-of-plane trajectory in the energy landscape of a 4-dipole system. The energy is plotted against θ, which is defined in the lower right inset. The magnetic configurations after energy minimization for $\theta = 0°$ and $\theta = 90°$ are also shown.*

The second trajectory is a path from configuration 4.b to 4.d. The final configuration is '3D', since the dipoles move out of the plane. The energy and the parametrization are given in figure 6. The energy attains a maximum at $\theta = 90°$, so the 3D configuration is only meta-stable. This is again in correspondence with the behaviour of the neocubes.

B. shape modifications

From figure 6 we conclude that the 3D configuration with 4 dipoles is not stable. In this paragraph it is investigated whether this 3D configuration can be made stable by modifying the shape of the particles. Moreover, if the energy of the 3D configuration can be reduced in this way, the 3D configuration might become energetically favourable over the 2D configurations.

Figure 7 illustrates a possible shape modification; the particles have been indented at three positions. With such a modification, the top particle can be positioned closer to the 3 bottom particles. This results in a lower

Figure 7: *Illustration of a shape modification. The unmodified particles (left drawing) can be indented to allow a closer packing of the spheres (right drawing). The exploded view (center drawing) shows the indentations and the vertical trajectory (line) of the top particle.*

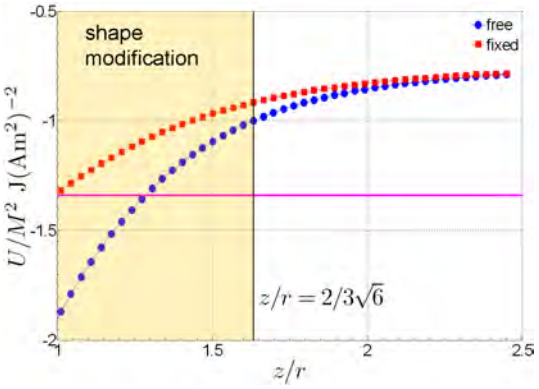

Figure 8: *Energy versus z position of the top dipole in the 3D configuration with 4 dipoles. In the 'free' case (circles) all dipoles were free rotate their dipole moment during the energy minimization; in the 'fixed' case (squares), the moment of the top dipole was fixed the z direction during the energy minimization. The shaded area indicates the region where the shape of the particles needs to be modified. The horizontal line indicates the energy of the 4-dipole ring configuration.*

energy.

The effect of this shape modification is investigated by simulating a trajectory. The 3 bottom dipoles are configured in a ring, with their centers in the *x*-*y* plane. The top particle moves vertically in the $-z$ direction, as illustrated in figure 7. At each position the energy is minimized and $U(z)$ is obtained, where z is the distance between the center of the top particle and the *x*-*y* plane. At $z/r = 2/3\sqrt{6}$ the top particle touches the bottom particles if the particles have their unmodified spherical shape. To allow a smaller z, the shape of the particles must be modified. Figure 8 shows the energies versus z/r that are obtained for two situations. In the first situation, all dipole moments are free to rotate. In the second situation, the magnetization of the top particle is fixed in the z direction. This is of interest, because the modification of the particles defines a preferred orientation of the dipole moment. However, the constraint of having preferred orientations of the dipole moments can be resolved by designing particles that contain magnets which are free to rotate with respect to the shell.

The energies of the two cases are compared with the 4-dipole ring configuration (4.b. in Table 1), since this is the 2D configuration with the lowest energy. In case that the top particle has a fixed magnetization in the z-direction, the energy is always larger than the energy of the ring configuration (horizontal line in figure 8). However, in the case where all particles are free to rotate their dipole moments, the energy is lower than the ring configuration if $z/r \leq 1.25$. Therefore, for particles with a rotatable magnet and a modified shape, the 3D configuration is preferred over the 2D configurations.

V – Conclusions

A 3D self-assembly system using milli-magnetic particles has been designed. The design allows the particles to hover freely in salt water.

The magnetostatic energies of simple particle configurations are obtained via simulations by dynamic minimization of this energy. The simulated energy barriers are in correspondence with the behaviour of the neocubes. Still, the accuracy of the simulations can be improved by taking into account the cylindrical shape of the magnets. In future experiments, the obtained energy barrier for the 3-dipole system might be validated.

Our simulations show that for 4-dipole systems a 2D configuration is energetically favoured over a metastable 3D structure. However, further simulations indicate that by modifying the shape of the particles it is possible to obtain stable 3D configurations. We will now focus on proving this exciting result experimentally. Furthermore, we will investigate the magnetic self-assembly of more intricate 3D architectures by clever design of the shape of the constituent particles.

References

[1] Miko Elwenspoek, Leon Abelmann, Erwin Berenschot, Joost van Honschoten, Henri Jansen, and Niels Tas. Self-assembly of (sub-)micron particles into supermaterials. *J. Micromech. Microeng.*, 20(6):064001, 2010.

[2] L. Abelmann, N. Tas, E. Berenschot, and M. Elwenspoek. Self-assembled three-dimensional nonvolatile memories. *Micromachines*, 1:1–18, 2010.

[3] John A. Pelesko. *Self assembly - The Science of Things That Put Themselves Together*. Chapman & Hall/CRC, 2007.

[4] David Vokoun, Marco Beleggia, Ludek Heller, and Petr Sittner. Magnetostatic interactions and forces between cylindrical permanent magnets. *Journal of Magnetism and Magnetic Materials*, 321(22):3758 – 3763, 2009.